Eur. Phys. J. A **7**, 287–291 (2000)

**THE EUROPEAN PHYSICAL JOURNAL A**



# Matter-induced $\omega \longrightarrow \pi\pi$ decay

W. Broniowski[1], W. Florkowski[1], B. Hiller[2]

[1] H. Niewodniczański Institute of Nuclear Physics, 31342 Kraków, Poland (e-mail: broniows@solaris.ifj.edu.pl, florkows@solaris.ifj.edu.pl)
[2] Center for Theoretical Physics, University of Coimbra, 3004 516 Coimbra, Portugal (e-mail: brigitte@malaposta.fis.uc.pt)

Received: 7 June 1999 / Revised version: 14 October 1999
Communicated by W. Weise

**Abstract.** We calculate the width for the $\omega \to \pi\pi$ decay in nuclear matter in a hadronic model including mesons, nucleons and $\Delta$ isobars. We find a substantial width of the longitudinally polarized $\omega$ modes, reaching $\sim 100$MeV for mesons moving suitably fast with respect to the nuclear medium.

**PACS.** 25.75.Dw relativistic heavy-ion collisions – 21.65.+f nuclear matter – 14.40.-n mesons

The dilepton measurements in the CERES [1] and HELIOS [2] experiments have indicated that the masses and/or widths of light vector mesons undergo large modifications in nuclear matter. Clearly, since the mesons interact strongly with the medium, this fact is not at all surprising. Indeed, in-medium modifications of hadron properties are predicted in a variety of theoretical calculations [3–16] (for a recent review see [17,18]). An interesting factor brought in by the presence of the medium is that processes which are forbidden in the vacuum by symmetry principles are now made possible. The constraints of Lorentz-invariance, $G$-parity, or isospin invariance in isospin-asymmetric media [19,20], are no longer effective. An example of such an "exotic" phenomenon which becomes possible and significant in the presence of nuclear matter is the decay of $\omega \to \pi\pi$. This process is, apart from a small isospin-violation effect, forbidden in the vacuum. [1] In this paper we show that the matter-induced width for this process is large. For $\omega$ moving with respect to the medium with a momentum above $\sim$ 200MeV (such momenta are easily accessible in heavy-ion collisions) the corresponding width, at the nuclear saturation density, is of the order of 100MeV. In addition, we find very different behavior of the longitudinally and transversely polarized $\omega$ mesons, with the former ones being much wider than the latter ones.

Our calculation is made in the framework of an effective hadronic theory. Mesons interact with the nucleons and $\Delta$ isobars, and the interactions are assumed to have the usual form used in many other calculations and fits. We work to the leading order in the nuclear density. Based on the experience of other in-medium calculations we hope that this approximation should be sufficient up to densities of the order of the nuclear saturation density. To this leading order only the diagrams shown in Fig. 1 contribute. In these diagrams the nucleon lines include the propagation of occupied states of the Fermi sea. The "bubble" diagram (a) has been analyzed by Wolf, Friman, and Soyeur in [21], where the role of the $\omega - \sigma$ mixing mechanism has been pointed out (see also [22,23]). In this process the $\omega$ meson is first converted, via interaction with the nucleons, into the scalar-isoscalar $\sigma$ meson, which in turn decays into two pions. The relevance of "triangle" diagrams (b) has been shown out in [24]. Note that in any formal counting scheme (low density, chiral limit, large number of colors) the diagrams (a) and (b) are of the same order and consistency requires to include both. Our present calculation of $\omega \to \pi\pi$ in nuclear matter includes a further contribution of diagrams (c-d) with the $\Delta(1232)$ isobar. Among other possible resonances, the $\Delta$ is the most important one due to the large value of the $\pi N\Delta$ vertex and small $\Delta - N$ mass splitting.

The solid line in Fig. 1 denotes the in-medium nucleon propagator, which can be conveniently decomposed in the free and density parts [25]

$$G(k) \equiv G_F(k) + G_D(k) \tag{1}$$
$$= (\not{k} + M)\left[\frac{1}{k^2 - M^2 + i\varepsilon} + \frac{i\pi}{E_k}\delta(k_0 - E_k)\theta(k_F - |\mathbf{k}|)\right],$$

where $k$ is the nucleon four-momentum, $M$ denotes the nucleon mass, $E_k = \sqrt{M^2 + \mathbf{k}^2}$, and $k_F$ is the Fermi momentum. The diagram (a) is non-zero only when one propagator is $G_D$, and the other one $G_F$. The only non-vanishing

[1] In the vacuum the partial width for the decay $\omega \to \pi^+\pi^-$ is only $\sim 0.2$MeV, and is due to the small isospin breaking and the resulting $\rho - \omega$ mixing. In this paper we are not concerned with this negligible effect.

Research supported by PRAXIS grants XXI/BCC/429/94 and PRAXIS/P/FIS/12247/1998, and by the Polish State Committee for Scientific Research grant 2P03B-080-12

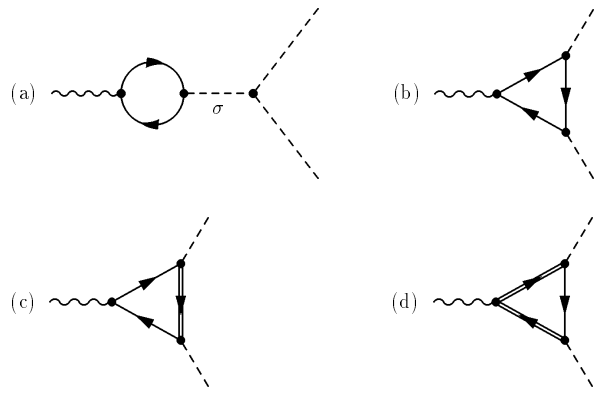


**Fig. 1.** Diagrams contributing to the $\omega \to \pi\pi$ amplitude in nuclear medium. The incoming $\omega$ has momentum $q$ and polarization $\epsilon$. The outgoing pions have momenta $p$ and $q-p$. Diagrams (b-d) have corresponding crossed diagrams, not displayed. The Feynman rules are given in the text

contributions in diagram (b) involve one $G_D$ propagator and two $G_F$ propagators. Diagram (a) involves the intermediate $\sigma$-meson propagator, which we take in the form

$$G_\sigma(k) = \frac{1}{k^2 - m_\sigma^2 + i\, m_\sigma \Gamma_\sigma - \frac{1}{4}\Gamma_\sigma^2}. \tag{2}$$

Here the mass and the width of the $\sigma$ meson are chosen in such a way that they reproduce effectively the experimental $\pi\pi$ scattering length at $q^2 = m_\omega^2 = (780\mathrm{MeV})^2$, which is the relevant kinematic point for the process at hand. From this fit we find $m_\sigma = 789$MeV and $\Gamma_\sigma = 237$MeV. Note that $m_\omega$ and $m_\sigma$ are very close to each other, which enhances the amplitude obtained from diagram (a) [21].

The double line in diagrams (c-d) denotes the $\Delta$ propagator

$$G_\Delta^{\alpha\beta}(k) = \frac{\not{k} + M_\Delta}{k^2 - M_\Delta^2 + i\, M_\Delta \Gamma_\Delta - \frac{1}{4}\Gamma_\Delta^2} \times \left[ -g^{\alpha\beta} + \frac{1}{3}\gamma^\alpha\gamma^\beta + \frac{2k^\alpha k^\beta}{3M_\Delta^2} + \frac{\gamma^\alpha k^\beta - \gamma^\beta k^\alpha}{3M_\Delta} \right]. \tag{3}$$

This formula corresponds to the usual Rarita-Schwinger definition [26,27] with the denominator modified in order to account for the finite width of the $\Delta$ resonance, $\Gamma_\Delta = 120$MeV.

We assume that the $\omega NN$ and $\omega\Delta\Delta$ vertices have the form which follows from the minimum-substitution prescription and vector-meson dominance applied to the nucleon and the Rarita-Schwinger [26] Lagrangians:

$$V_{\omega NN}^\mu = g_\omega \gamma^\mu, \qquad V_{\omega\Delta\Delta}^{\mu\alpha\beta} = g_\omega \left[ -\gamma^\mu g^{\alpha\beta} + g^{\alpha\mu}\gamma^\beta + g^{\beta\mu}\gamma^\alpha + \gamma^\alpha\gamma^\mu\gamma^\beta \right]. \tag{4}$$

Possible anomalous couplings can be incorporated at the expense of having more parameters. The results presented below do not depend qualitatively on the form of the coupling, as long as it remains strong. The coupling constant $g_\omega$ can be estimated from the vector dominance model. We use $g_\omega = 9$. For the $\pi NN$ vertex we use the pseudoscalar coupling, with the coupling constant $g_{\pi NN} = 12.7$. The same value is used for $g_{\sigma NN}$. The $\sigma\pi\pi$ coupling constant is taken to be equal to $g_{\sigma\pi\pi} = 12.8\, m_\pi$, where $m_\pi = 139.6$MeV is the physical pion mass (this value follows from the fit done to $\pi\pi$ scattering phase shifts done in [21]). The $\pi N\Delta$ vertex has the form $V_{\pi N\Delta}^\mu = (f_{\pi N\Delta}/m_\pi) p^\mu \boldsymbol{T}$, where $p^\mu$ is the pion momentum, $\boldsymbol{T}$ is the $\frac{1}{2} \to \frac{3}{2}$ isospin transition matrix, and the coupling constant $f_{\pi N\Delta} = 2.1$ [28]. [2]

The amplitude, evaluated according to the diagrams depicted in Fig. 1 (a-d) can be uniquely decomposed in the following Lorentz-invariant way:

$$\mathcal{M} = \epsilon^\mu (A p_\mu + B u_\mu + C q_\mu), \tag{5}$$

where $p$ is the four-momentum of one of the pions, $q$ is the four-momentum of the $\omega$ meson, $u$ is the four-velocity of nuclear matter, and $\epsilon$ specifies the polarization of $\omega$. Our calculation is performed in the rest frame of nuclear matter, where $u = (1,0,0,0)$. In this reference frame the amplitude $\mathcal{M}$ vanishes for vanishing 3-momentum $\mathbf{q}$, as requested by rotational invariance. Hence, the process $\omega \to \pi\pi$ occurs only when the $\omega$ moves with respect to the medium.

The expression for the decay width reads

$$\Gamma = \frac{1}{2} 3 \frac{1}{n_s} \sum_s \frac{1}{2q_0} \int \frac{d^3p}{(2\pi)^3 2p_0} \int \frac{d^3p'}{(2\pi)^3 2p_0'} \times |\mathcal{M}|^2 (2\pi)^4 \delta^{(4)}(q - p - p'), \tag{6}$$

where the factor $\frac{1}{2}$ is the symmetry factor when the decay proceeds into two neutral pions, the factor of 3 accounts for the isospin degeneracy of the final pion states (*i.e.* neutral and charged pions), $n_s$ is the number of spin states of the $\omega$ meson, and $\sum_s$ denotes the sum over these spin states ($q$ , $p$ and $p' = q - p$ are the four-momenta of the $\omega$ meson, and the two pions, respectively).

We take the effort to analyze separately the longitudinally and transversely polarized $\omega$, since the presence of the medium results in different behavior of these states. Transversely polarized $\omega$ has two helicity states ($n_s = 2$), with projections $s = \pm 1$ on the direction of $\mathbf{q}$, and the longitudinally polarized $\omega$ has one helicity state ($n_s = 1$), with the corresponding projection $s = 0$. An explicit calculation yields

$$\sum_{s=\pm 1} \varepsilon_{(s)}^\mu \varepsilon_{(s)}^{*\nu} \equiv -T^{\mu\nu} = = \frac{(q^\mu - q\cdot u\ u^\mu)(q^\nu - q\cdot u\ u^\nu)}{q\cdot q - (q\cdot u)^2} - g^{\mu\nu} + u^\mu u^\nu, \varepsilon_{(s=0)}^\mu \varepsilon_{(s=0)}^{*\nu} \equiv -L^{\mu\nu} = = -\frac{(q^\mu - q\cdot u\ u^\mu)(q^\nu - q\cdot u\ u^\nu)}{q\cdot q - (q\cdot u)^2} + \frac{q^\mu q^\nu}{q\cdot q} - u^\mu u^\nu. \tag{7}$$

[2] There is another possible structure in the $\pi N\Delta$ coupling, of the form $a \not{p} \gamma^\mu$. Our vertex corresponds to the popular choice of the off-shell parameter $a$ set to zero.

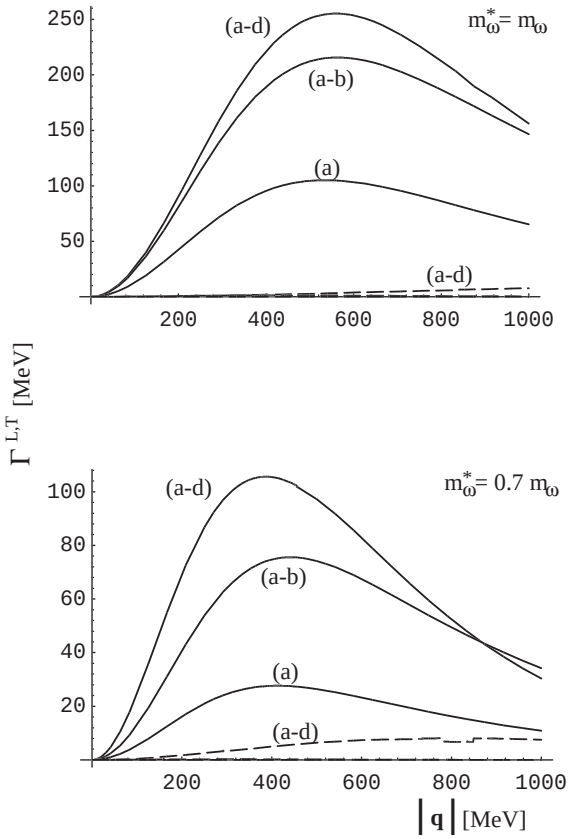


**Fig. 2.** The in-medium width of the $\omega$ meson plotted as a function of its 3-momentum $|\mathbf{q}|$ for density equal to the nuclear saturation density. The solid (dashed) lines correspond to the longitudinal (transverse) mode. The labels (a), (a-b) and (a-d) refer to Fig. 1. They indicate the diagrams included in the calculation: (a) $\omega - \sigma$ mixing mechanism, (a-b) $\omega - \sigma$ mixing together with the "triangle" nucleon diagrams, (a-d) the full result, including the contribution from the $\Delta$ isobar

The tensors $T^{\mu\nu}$ and $L^{\mu\nu}$ are defined in such a way that they are projection operators. In addition, $T^{\mu\nu}q_\nu = 0$ and $L^{\mu\nu}q_\nu = 0$, which reflects current conservation, and $T^{\mu\nu}u_\nu = 0$. From relations (5) and (7) in (6) we find that

$$|\mathcal{M}_T|^2 = |A|^2 p_\mu(-T^{\mu\nu})p_\nu, \qquad (8)$$
$$|\mathcal{M}_L|^2 = (A^* p_\mu + B^* u_\mu)(-L^{\mu\nu})(Ap_\nu + Bu_\nu).$$

Note that the value of the coefficient $C$ is irrelevant for our calculation. For the diagram (a) we find $A = 0$, $B \neq 0$, hence this diagram contributes only to the width of the longitudinal mode. Diagrams (b-d) have $A \neq 0$, $B \neq 0$, and contribute to the width of both the longitudinal and transverse modes.

As we have said, we evaluate the amplitude $\mathcal{M}$ to leading order in the baryon density. This leads to a simplification. The integrals of the form $\int_0^{k_F} k^2 dk\, f(k)$ arising in our calculation are replaced by $f(0)\int_0^{k_F} k^2 dk$, which is proportional to baryon density, $\rho_B$. Consequently, the widths $\Gamma^{L,T} \sim \rho_B^2$.

In Fig. 2 we present our numerical results at the nuclear saturation density, $\rho_B = \rho_0 = 0.17\mathrm{fm}^{-3}$. We show $\Gamma^L$ (solid lines) and $\Gamma^T$ (dashed lines) plotted as functions of $|\mathbf{q}|$. The upper part of the plot is for $m^*_\omega = m_\omega = 780$MeV, i.e. the value of the $\omega$ mass is not modified by the medium. The lower part is for $m^*_\omega = 0.7 m_\omega$. In both cases we reduce the value of the in-medium nucleon mass to 70 % of its vacuum value, $M^* = 0.7M$, which is a typical number at the nuclear saturation density. We also reduce by the same factor the mass of the $\Delta$, *i.e.* $M^*_\Delta = 0.7 M_\Delta$, since it is expected to behave similarly to the nucleon. The labels indicate which diagrams of Fig. 1 have been included. The complete result corresponds to the case (a-d). The case (a) reproduces the result of [21] [3]. We note that the inclusion of subsequent processes of Fig. 1 substantially increases the result. All the curves start as $\mathbf{q}^2$ at low $|\mathbf{q}|$. The longitudinal width reaches a maximum at $|\mathbf{q}| \sim$ a few hundred MeV, and the value at the peak is large: 250MeV for $m^*_\omega = m_\omega$ and 100MeV for $m^*_\omega = 0.7 m_\omega$. The transverse width is strictly zero with diagram (a), less than 1MeV with diagrams (a-b), reach a few MeV when the diagrams with the $\Delta$ are included. Qualitatively similar results follow for other choices of parameters. One should bare in mind that the effect is proportional to $\rho_B^2$, hence may be much larger at higher densities.

Next, we discuss the temperature dependence of our results. This is important, since in heavy-ion collisions we are faced with temperatures $T \sim 150$MeV. Finite $T$ affects our calculation by 1) the presence of a Bose-Einstein enhancement factor in the formula (6), and 2) by implicit dependence of hadronic parameters on $T$. Effect 1) supplies the formula (6) with a factor of $1 + f_\pi(p) + f_\pi(p')$ in the phase-space integrand, where $f_\pi(p) = (\exp(p_0/T) - 1)^{-1}$ is the pion distribution function [29] . Its presence raises $\Gamma^L$ by $5 - 10\%$ at $T = 100$MeV, and by $15 - 25\%$ at $T = 150$MeV, depending on the values of the in-medium nucleon and $\omega$ masses.

Effect 2) can be read-off from Fig. 3. This is because finite $T$ modifies the values of $M^*$, $M^*_\Delta$, $m^*_\omega$. We take no prejudice as to what these modifications are, and show the results for values of $M^*/M = M^*_\Delta/M_\Delta$ ranging from 0.7 to 1, and for two values of $m^*_\omega$. For the case of the full calculation (diagrams (a-d) in Fig. 1) Fig. 3 shows a drop of $\Gamma^L$ by about a factor of 2 as we go with $M^*/M$ from 0.7 to 1. The calculation without the $\Delta$ displays a drop by a about factor of 4. Nevertheless the widths even at $M^*/M = 1$ remain substantial, also in view of the effect 1) discussed above.

Our main conclusions are: 1) nuclear matter induces the $\omega \to \pi\pi$ transitions with large partial widths, 2) the widths depend strongly on the three momentum of the $\omega$ with respect to the medium, $|\mathbf{q}|$, 3) the longitudinal mode is much wider than the transverse mode.

The results obtained mean that in a hadron gas, such as created in a heavy-ion collision, the propagation of longitudinally polarized $\omega$ meson is inhibited when the momentum $|\mathbf{q}|$ is nonzero. This will cause a depletion in the

[3] Since the width of the longitudinal modes is much larger than the width of the transverse modes, the width averaged over polarizations, such as calculated in [21], is nearly equal to one third of our longitudinal width.

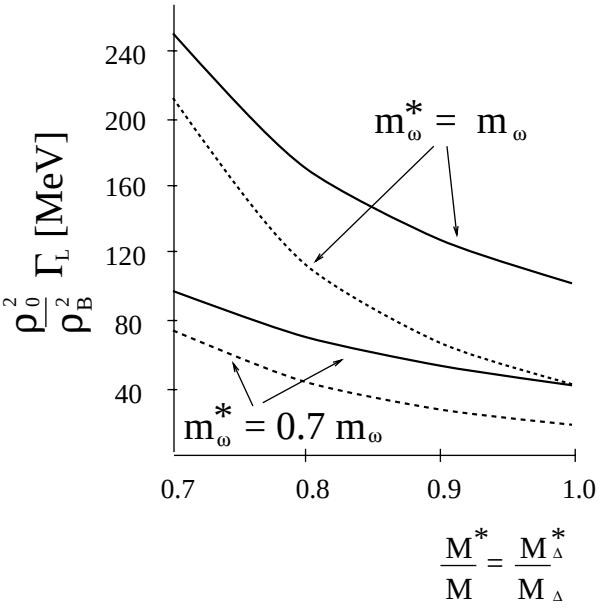


**Fig. 3.** The dependence of the longitudinal width $\Gamma_L$ at $|\mathbf{q}| = 500$MeV on the ratio $M^*/M = M^*_\Delta/M_\Delta$ for two different values of $m^*_\omega$, and for density equal to the nuclear saturation density. Solid lines: the full calculation, with diagrams (a-d) of Fig. 1, dashed lines: the calculation with diagrams (a-b) of Fig. 1

population of the $\omega$ mesons. Such processes should be included in simulations of heavy-ion collisions. In fact, the results of some recent transport calculations [30] show an excess in the dilepton yield at $q^2 = m^2_\omega$, attributed to the direct $\omega \to e^+e^-$ decay. With an increased hadronic width of the $\omega$ a better agreement with the data may be achieved.

The important question is to what extent can the discussed process influence shape of the dilepton-production cross-sections in relativistic heavy-ion collisions. Our results can be used to calculate the cross section for the $\pi\pi$ annihilation into dileptons occurring in the $\omega$ channel. This mechanism has been analyzed for the first time in [21]. The calculation of the annihilation cross section requires the knowledge of the same amplitude that has been used in the calculation of the omega width, see Fig. 4. In [21] only the $\omega-\sigma$ mixing term was included in this amplitude (diagram (a) of Fig. 1). In our present calculation we take into account additional diagrams shown in Figs. 1 (b) - (d). Moreover, we take into consideration differences in the propagation of the transverse and longitudinal modes, which is important due to the large difference observed in the widths.

The $\pi\pi$ annihilation cross section corresponding to Fig. 4, averaged over the incoming pion momenta at fixed total four-momentum $q = (q^0, \mathbf{q})$, can be written in the compact form

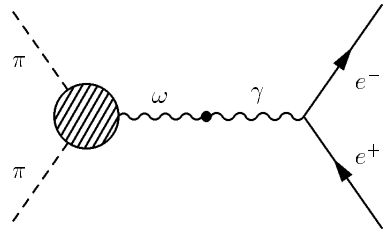


**Fig. 4.** Pion annihilation process in the $\omega$ channel. The blob corresponds to the amplitude shown in Fig. 1, and the dot denotes the vector-meson-dominance conversion factor $em^2_\omega/(2g_\omega)$

$$\sigma = \frac{8\pi^2 q^0 m^4_\omega}{9q^2(q^2/4 - m^2_\pi)} \left(\frac{\alpha}{g_\omega}\right)^2 \left(2|G^T_\omega|^2 \Gamma^T + |G^L_\omega|^2 \Gamma^L\right), \tag{9}$$

where

$$|G^{T,L}_\omega|^2 = \frac{1}{[q^2 - m^2_\omega - \frac{1}{4}\gamma^2(\Gamma_0 + \Gamma^{T,L})^2]^2 + \gamma^2 m^2_\omega (\Gamma_0 + \Gamma^{T,L})^2} \tag{10}$$

is the modulus of the $\omega$ propagator squared. The Lorentz $\gamma$ factor arises since all widths are evaluated in the rest frame of the medium. The widths $\Gamma^T$ and $\Gamma^L$ should be calculated in the way described above with the only difference that the physical mass of $\omega$ is now replaced by the invariant dilepton mass $\sqrt{q^2}$. The quantity $\Gamma_0$ denotes the width of the $\omega$ due to all other processes, such as $\omega \to \pi\pi\pi$, $\omega N \to \pi N$, *etc.*, which are not considered here (see for example [12,15]). With $\Gamma_0 \sim 10$MeV [12] and our values for $\Gamma^{T,L}$ we obtain the cross section from (9), which is typically a fraction of a microbarn. With larger values of $\Gamma_0$ the cross section drops according to (9). Our number is to be compared to a few microbarns from the decay via the $\rho$ resonance [21]. The formula (9) is given for $T = 0$. At finite $T$ it is modified by the presence of the product of the pion distribution functions in the average over the initial two-pion states. However, we have checked that this influences the result at the level of a few per cent for $T$ up to 150MeV and $|\mathbf{q}|$ up to 500MeV.

If the dilepton-production experiments measured the three-momentum $\mathbf{q}$ of the dilepton pair coming from a vector-meson decay, then they should observe different behavior at different values of $|\mathbf{q}|$. Such measurement would be very helpful for a better understanding of meson dynamics in the nuclear medium.

Our last remark refers to the final state interactions, which can be important [28]. The pions emitted in processes of Fig. 1 can interact in the final channel. This will result in an appropriate modification the $\omega \to \pi\pi$ amplitude. The full analysis of the final-state interactions requires a model for the $\pi\pi$ scattering amplitude, as well as solving a Lipmann-Schwinger equation. This is beyond the scope of this paper. Note, however, that the diagram (a), which includes the intermediate $\sigma$ state, does in fact account for final-state interactions. In this process the pions form a resonance in the $S$-channel, which enhances

the amplitude. Similar rescattering can also occur for the diagrams (b-d). Thus, the final-state interactions are only partially included in our analysis.

We thank Bengt Friman for numerous valuable comments and for the suggestion to include the $\Delta$ in the presented analysis.

## References

1. CERES Collab., G. Agakichiev *et al.*, Phys. Rev. Lett. **75** (1995) 1272
2. HELIOS/3 Collab., M. Masera *et al.*, Nucl. Phys. **A590** (1995) 3c
3. G. E. Brown and M. Rho, Phys. Rev. Lett. **66** (1991) 2720
4. L. S. Celenza, A. Pantziris, and C. M. Shakin, Phys. Rev. **C45** (1992) 205
5. T. Hatsuda and S. H. Lee, Phys. Rev. **C46** (1993) R34
6. H.-C. Jean, J. Piekarewicz, and A. G. Williams, Phys. Rev. **C49** (1994) 1981
7. W. Cassing, W. Ehehalt, and C. M. Ko, Phys. Lett. **B363** (1995) 35
8. G. Q. Li, C. M. Ko, and G. E. Brown, Nucl. Phys. **A606** (1996) 568
9. T. Hatsuda, H. Shiomi, and H. Kuwabara, Prog. Theor. Phys. **95** (1996) 1009
10. R. Rapp, G. Chanfray, and J. Wambach, Nucl. Phys. **A617** (1997) 472
11. B. Friman and H. J. Pirner, Nucl. Phys. **A617** (1997) 496
12. F. Klingl, N. Kaiser, and W. Weise, Nucl. Phys. **A624** (1997) 527
13. S. Leupold, W. Peters, and U. Mosel, Nucl. Phys. **A628** (1998) 311
14. V. L. Eletsky, B. L. Ioffe, and J. I. Kapusta, Eur. J. Phys. **A3** (1998) 381
15. B. Friman, Acta Phys. Pol. **B29** (1998) 3195
16. E. L. Bratkovskaya and C. M. Ko, Phys. Lett. **B445** (1999) 265
17. *Hadrons in Nuclear Matter*, edited by H. Feldmeier and W. Nörenberg (GSI, Darmstadt, 1995), proc. Int. Workshop XXIII on Gross Properties of Nuclei and Nuclear Excitations, Hirschegg, Austria, 1995
18. *Quark Matter 97*, proc. 13th Int. Conf. on Ultra-Relativistic Nucleus-Nucleus Collisions, Tsukuba, Japan, 1997, Nucl. Phys. **A638**, and references therein
19. A. K. Dutt-Mazumder, B. Dutta-Roy, and A. Kundu, Phys. Lett. **B399** (1997) 196
20. W. Broniowski and W. Florkowski, Phys. Lett. **B440** (1998) 7
21. G. Wolf, B. Friman, and M. Soyeur, Nucl. Phys. **A640** (1998) 129
22. T. Kunihiro, Prog. Theor. Phys. Suppl. **120** (1995) 75
23. D. Blaschke, Yu. L. Kalinovsky, S. Schmidt, and H.-J. Schulze, Phys. Rev. **C 57** (1998) 438
24. W. Broniowski, W. Florkowski, and B. Hiller, Acta Phys. Pol. **B30** (1999) 1079
25. S. A. Chin, Ann. Phys. (NY) **108** (1977) 301
26. W. Rarita and J. Schwinger, Phys. Rev. **60** (1941) 61
27. M. Benmerrouche, R. Davidson, and N. C. Mukhopadhyay, Phys. Rev. **C39** (1989) 2339
28. J. W. Durso, A. Jackson, and B. VerWest, Nucl. Phys. **A345** (1980) 471
29. P. Koch, Zeit. f. Physik **C57** (1993) 283
30. V. Koch, Proc. of the XXXVII International Winter Meeting on Nuclear Physics, Bormio, Italy, January 1999, nucl-th/9903008